34th Annual International Conference of the IEEE EMBS
San Diego, California USA, 28 August - 1 September, 2012

Experimental Observations on the Human Arm Motion Planning under an Elbow Joint Constraint

Hyosang Moon, *Student Member, IEEE,* Nina P. Robson, *Member, IEEE,*
Reza Langari, *Senior Member, IEEE* and John J. Buchanan

Abstract— **This paper seeks to define the governing strategies by which the human central nervous system (CNS) finds optimal solutions for an arm reaching motion, when an elbow joint is constrained. The compensated arm reaching motion under the joint kinematic constraint is observed by human experiments. We present an experimental protocol, where subjects perform point-to-point reaching tasks with a lightweight elbow brace to restrict the elbow kinematics with minimal effect on the arm dynamics. The human compensatory strategy is analyzed in terms of hand path kinematics (i.e. spatial and temporal characteristics) and the arm postural configuration. The spatial and temporal characteristics of hand path are approximated by the Euclidean geodesic curves and the well known bell–shaped smooth profile, respectively. Furthermore, the contribution of each joint degree–of–freedom (DOF) motion is discussed and its relation to the arm posture selection is elaborated.**

I. Introduction

Humans perform versatile reaching motions in daily activities to achieve complex desired position and orientation of their hands (i.e. end–effectors) even under unusual environments. It seems that the central nervous system (CNS) enables such optimal and robust motions through interconnected motion planning, control and learning mechanisms within it. One of the main interests in the issue of motor neuroscience can be described by Bernstein's question: how does the CNS solve the redundant problem of motor control without conscious effort to complete skillful actions [1]. From many experimental observations, it is generally accepted that human motion is controlled by governing rules which induce a finite set of preferred patterns (e.g. the tendency for synchronizing interlimb coordination [2]). In a hierarchical control strategy, reaching is planned with respect to the hand kinematics and motion planning processes are separate from motion execution processes [3]. This viewpoint supports the idea that there are simple governing rules for motion planning. Since the disturbances and uncertainties on the plant model (e.g. time varying body dynamics, disturbances in the neural signal and varying actuator dynamics due to muscle fatigue) are separated from the motion planning process, the governing rule can keep its simplicity. The governing rules for reaching and pointing actions have been identified in multiple studies. Morasso's research [4] supports the idea that point–to–point reaching motions have consistent characteristics, such as a straight path with a bell–shaped velocity profile. Flash and Hogan [5] formulates a so–called minimum jerk model to approximate the voluntary hand movements in a 2D plane and verified their model by experimental observations. Biess *et al*. [6] model 3D arm pointing movements as a geodesic curve in the joint coordinates with respect to the kinetic energy metric in the Riemannian configuration space. It seems that the consistent motion planning strategy is applied to the motion with the kinematic constraints on the hand with some modifications. In their study of arm reaching on a constrained hemispheric force field, Sha *et al*. [7] showed that hand paths approach a geodesic curve through training. Liebermann *et al*. [8] performed similar experiments with a kinematic constraint on the hand path using a mechanical linkage system and concluded that the hand does not follow a geodesic curve exactly, but does preserve a bell–shaped velocity profile.

This paper seeks to define human arm motion planning under a kinematic constraint on the elbow joint. Since the joint constraint reduces the arm mobility itself, it induces more challenging inverse kinematics problem when the CNS specifies the commands for each joint degree–of–freedom (DOF). The hypothesized strategy is compared with the experimental results in terms of hand paths kinematics (i.e. spatial and temporal characteristics). Preliminary observations on the arm postural configuration along the motion are also discussed.

II. Methodology

A. Human Arm Kinematics

Human arm kinematics can be simplified as a seven DOFs serial chain (i.e. 3 DOFs shoulder, 1 DOF elbow and 3 DOFs wrist joint). Shoulder and elbow joint motion position the hand in space, while wrist joint motion defines hand orientation. In this paper, only the position of the hand is specified, without any specifications of orientation, to focus on the reaching task. Therefore the wrist joint DOFs are excluded from the human arm model and hand location is defined as the position of the wrist center. When the human arm is subjected to an elbow failure, the arm's kinematic structure becomes a serial SS (Spherical – Spherical) kinematic chain, characterized by a spherical workspace, centered at the shoulder. The reconfigured SS chain is assumed to be a virtual rigid link with a length r that connects the shoulder (center of the sphere) and the hand. The three independent DOFs of the virtual link are defined as latitude θ,

Hyosang Moon and Reza Langari are with the Department of Mechanical Engineering, Texas A&M University, College Station, TX 77843 USA (e-mail: {hsmoon, rlangari}@ neo.tamu.edu).

Nina P. Robson is with the Department of Mechanical Engineering, California State University Fullerton, Fullerton CA 92843 USA and the Department of Engineering Technology and Industrial Distribution, Texas A&M University, College Station, TX 77843 USA (e-mail: robson@entc.tamu.edu).

John J. Buchanan is with the Department of Health and Kinesiology, Texas A&M University, College Station, TX 77843 USA (e-mail: jbuchanan@hlkn.tamu.edu).

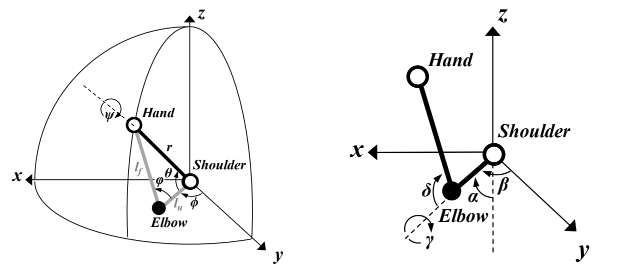

(a) Explicit angular coordinates (b) Joint coordinates
Figure 1. Kinematic model of the human arm in each coordinate system

longitude ϕ and roll ψ as shown in Figure 1(a). The hand location can be represented by the forward kinematics with respect to the explicit angular coordinates as:

$$f_E(\theta,\phi,\psi) = \begin{bmatrix} x_h(\theta,\phi) \\ y_h(\theta,\phi) \\ z_h(\theta,\phi) \end{bmatrix} = \begin{bmatrix} r\cos\theta\sin\phi \\ r\cos\theta\cos\phi \\ r\sin\theta \end{bmatrix}, \tag{1}$$

or with respect to the joint coordinates, i.e. shoulder azimuth α, elevation β, axial rotation γ and elbow flexion δ, as [6]:

$$f_J(\alpha,\beta,\gamma,\delta) = \begin{bmatrix} x_e \\ y_e \\ z_e \end{bmatrix} + \begin{bmatrix} l_f\{s_\delta(c_\alpha s_\beta c_\gamma - c_\beta s_\gamma) + s_\alpha s_\beta c_\delta\} \\ l_f\{s_\delta(c_\alpha c_\beta c_\gamma + s_\beta s_\gamma) + s_\alpha c_\beta c_\delta\} \\ l_f(s_\alpha c_\gamma s_\delta - c_\alpha c_\delta) \end{bmatrix}. \tag{2}$$

Here, $s_{(.)} = \sin(.)$, $c_{(.)} = \cos(.)$ and the link length of upper arm and forearm are referred as l_u and l_f, respectively. The elbow position in (2) is obtained as:

$$\mathbf{x_e} = \begin{bmatrix} x_e \\ y_e \\ z_e \end{bmatrix} = \begin{bmatrix} l_u\sin\alpha\sin\beta \\ l_u\sin\alpha\cos\beta \\ -l_u\cos\alpha \end{bmatrix}. \tag{3}$$

For clarity, refer to Figure 1(b). Note that the elbow angle δ is constant. On the other hand, the explicit angles can be computed from the hand position $\mathbf{x_h}(x_h, y_h, z_h)^T$ and the elbow position $\mathbf{x_e}(x_e, y_e, z_e)^T$ in the Cartesian coordinates as:

$$\theta = \operatorname{asin}\left(\frac{z_h}{r}\right), \tag{4}$$

$$\phi = \operatorname{atan2}(x_h, y_h). \tag{5}$$

The roll ψ is derived as the angle of arm plane with respect to the vertical plane [9]:

$$\psi = \operatorname{sign}\left[(\mathbf{n_v} \times \mathbf{n_{ap}}) \cdot \ \mathbf{n}\right] \ldots (\ \mathbf{v} \ \ \mathbf{ap}) \tag{6}$$

The normal unit vectors to the vertical plane and the arm plane, $\mathbf{n_v}$ and $\mathbf{n_{ap}}$, are derived as:

$$\mathbf{n_v} = \frac{\mathbf{u_{-z}} \times \mathbf{x_h}}{\|\mathbf{u_{-z}} \times \mathbf{x_h}\|} \quad \text{and} \quad \mathbf{n_{ap}} = \frac{\mathbf{x_e} \times \mathbf{x_h}}{\|\mathbf{x_e} \times \mathbf{x_h}\|}. \tag{7}$$

where $\mathbf{u_{-z}}$ represents the unit vector directing negative z direction. The joint angles can be obtained through the inverse kinematics [6]:

$$\alpha = \operatorname{acos}\left(\frac{-z_e}{l_u}\right), \tag{8}$$

$$\beta = \operatorname{atan2}(x_e, y_e), \tag{9}$$

$$\gamma = \operatorname{atan2}\left(l_u(x_e y_h - x_h y_e),\, y_e(y_e z_h - y_h z_e) - x_e(z_e x_h - z_h x_e)\right), \tag{10}$$

$$\delta = \operatorname{acos}\left(\frac{x_h^2 + y_h^2 + z_h^2 - l_u^2 - l_f^2}{2 l_u l_f}\right). \tag{11}$$

B. Hypothesis on the Human Strategy

The current paper is based on the hypothesis that the governing rule of human arm motion planning is consistent even under the joint kinematic constraints, i.e. the hand path follows the shortest path with a bell–shaped velocity profile. We hypothesize that the CNS plans compensatory hand paths on the constrained workspace as the shortest path through a subject's visual field which becomes the Euclidean geodesic curve in the Cartesian coordinate system. The Euclidean geodesic equations on the spherical workspace are derived in terms of the redefined explicit angular coordinates $u=[\theta, \phi]^T$ with respect to the time as:

$$\ldots \ [\ \ ij\ ] \tag{12}$$

where Γ_{ij} is the Christoffel Symbols of the second kind. Note that the hand location is independent of the roll ψ (see (1)). The equivalent set of equations is represented as:

$$\ddot{\theta} + \dot{\psi}^2 \sin\theta\cos\theta = 0, \quad \ddot{\psi} - 2\dot{\theta}\dot{\psi}\tan\theta = 0. \tag{13}$$

The integral curve obtained from (13) becomes the Euclidean geodesic on the sphere. It is well known that the geodesic on a sphere is the great circle which connects the two target points on the surface.

Once the geometric shape of the hand's path is determined, the path is segmented into small pieces as a real–time reference trajectory according to a temporal strategy. In this stage, it is considered that the CNS forms a smooth bell–shaped velocity profile which can be approximated by the output of a minimum jerk model. In order to keep the geometric shape of the hand path, the cost function of the minimum jerk model is modified in terms of arc length along the hand path [6], by:

$$J = \int_0^{t_f} \dddot{s} \ldots \tag{14}$$

where s is the arc length as a function of time t, and t_f refers the total movement time.

C. Experimental Setup

In order to verify our hypothesis on human movement planning strategy with a joint constraint, arm reaching experiments with an elbow restriction are designed. To realize the joint kinematic constraints with minimal effects on arm dynamics, light weight wrist and elbow braces were utilized (AirCast A2 Wrist Stabilizing Brace and AirCast

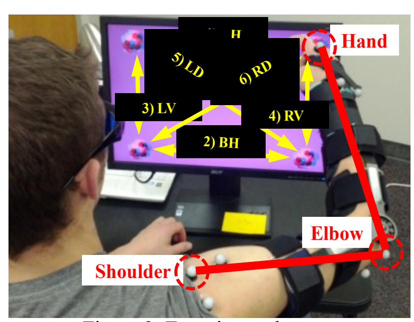

Figure 2. Experimental setup.

Mayo Elbow Brace, DJO Global Inc., USA). The elbow joint angle was fixed first at 30º and then at 60º of flexion where 0º indicates full extension. Five subjects (4 males and 1 female, all right handed) participated in the experiments. Participants' trunk motion was restrained on a high–back chair by elastic bands. Four target points were displayed on a computer monitor and six reaching tasks were defined (see Figure 2): 1) top horizontal (TH), 2) bottom horizontal (BH), 3) left vertical (LV), 4) right vertical (RV), 5) left diagonal (LD), and 6) right diagonal (RD). For enhancing the subjects' visual perception, stereoscopic target image was applied. In each trial, the subject performed reaching motion from the initial to the final targets and traveled back to the initial one. The initial target was always decided as the left most and upper most one in each task. Reflective markers were placed on the shoulder, elbow and wrist (see Figure 2) and the 3D position of the markers was captured with a 3 camera Vicon Motion Capture System (Vicon, OMGPlc., UK).

III. Experimental Results

A. Hand Paths Geometry with an Elbow Joint Constraint

The hand paths were compared to Euclidean geodesic curves. Selected examples of hand paths are shown in Figure 3 ((a) TH, (b) LV and (c) LD reaching motions with 60º elbow restriction, all in the forward direction). As presented in the figure, the hand paths closely follow the geodesics regardless of the reaching direction. For the quantitative analysis, hand path length index (HPLI) was defined as:

$$\text{HPLI} = \frac{L_{EXP} - L_{GEO}}{L_{GEO}} \times 100(\%) \qquad (15)$$

with L_{EXP} and L_{GEO} the arc lengths of the experimental hand path and geodesic, respectively. HPLI values for all participants are averaged and presented in Figure 5(a). In the forward motions, the deviations between the actual hand path and the geodesics are mostly within 5% in terms of arc length regardless of reaching directions.

B. Hand Speed Profile with an Elbow Joint Constraint

The speed profiles of the experimental data were normalized and compared to the minimum jerk model output. For smoothing the speed data, a zero phase low–pass filter was applied (3rd order Butterworth, 6.4 Hz cutoff frequency). The minimum jerk speed profile is uni–modal and symmetric bell shape. According to the study of Richardman and Flash

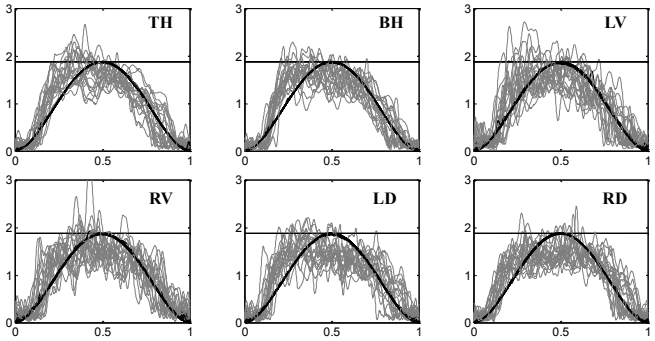

Figure 4. Normalized hand speed profile comparison: the abscissa and ordinate of each graph refer normalized time frame τ and the scaled speed with respect to the average speed. The black thick lines indicate the minimum jerk model output while the thinner grey lines represent the actual hand speed. The dotted grid shows the line of the ideal ration value

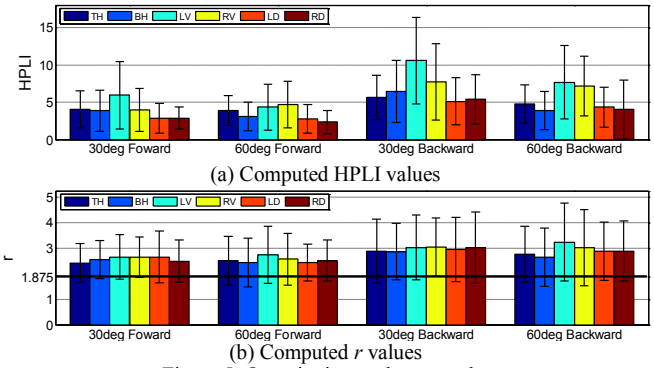

(a) Computed HPLI values

(b) Computed r values

Figure 5. Quantitative analyses results

[10] for an unconstrained arm, the minimum jerk model has the ratio $r = v_{peak}/v_{avg} = 1.875$. As an example, Figure 4 compares experimental results of a selected subject with the minimum jerk model outputs. In the figure, most of the hand speed profiles roughly approximate the shape of minimum jerk model output. The ratio r values are computed and averaged across all subjects (see Figure 5(b)). According to the r values, the averaged experimental data shows more agile motions than the minimum jerk model output.

C. Preliminary Observations on the Arm Posture with an Elbow Joint Constraint

Once the hand path is determined, the arm posture can be varied by the elbow location around the virtual link (see Figure 1) [6]. Therefore, the explicit angular DOFs can be functionally classified: the latitude θ and the longitude ϕ govern the hand path while the roll ψ dominates the arm

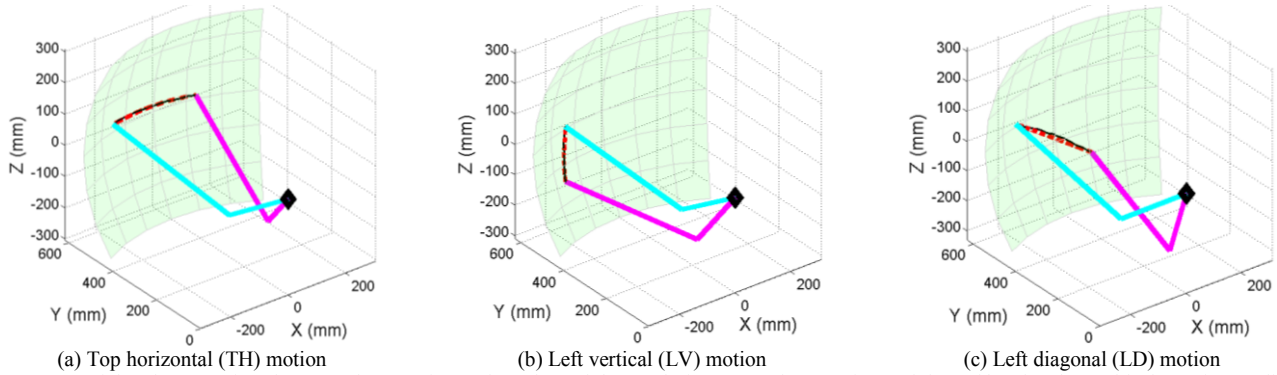

(a) Top horizontal (TH) motion (b) Left vertical (LV) motion (c) Left diagonal (LD) motion

Figure 3. Spatial path comparison between the experimental results and the geodesic curves: the experimental data of hand paths are black continuous lines while the geodesic curves are red dashed lines. The spherical workspace (shaded region) is presented for a better understanding. Black diamond represents the shoulder location, cyan and magenta links indicate the initial and final arm posture configurations, respectively.

posture. Note that ψ is the only explicit angular DOF independent of the forward kinematics (see (1)). In order to observe the arm postural configuration, a mapping F, from the joint DOFs to the explicit angular DOFs, is defined as:

$$F(\alpha,\beta,\gamma,\delta)=\begin{bmatrix}\theta(\alpha,\beta,\gamma,\delta)\\ \phi(\alpha,\beta,\gamma,\delta)\\ \psi(\alpha,\beta,\gamma,\delta)\end{bmatrix}. \quad (16)$$

The sensitivity of the mapping F is derived by the Jacobian,

$$J(F)=\begin{bmatrix}\frac{\partial F}{\partial\alpha} & \frac{\partial F}{\partial\beta} & \frac{\partial F}{\partial\gamma} & \frac{\partial F}{\partial\delta}\end{bmatrix}, \quad (17)$$

and the contribution of each joint DOF on the hand path formulation (i.e. latitude θ and longitude ϕ) and the arm posture selection (i.e. roll angle ψ) is quantified by

$$\frac{d\Theta}{dt}=J(F)\frac{d\mathrm{A}}{dt} \quad (18)$$

where $\Theta=[\theta,\phi,\psi]^{\mathrm{T}}$, $\mathrm{A}=[\alpha,\beta,\gamma,\delta]^{\mathrm{T}}$ and t indicates the time variable. Figure 6(a–c) represents the computed joint DOF contributions for a selected subject's top horizontal (TH) reaching trial with 60º elbow. Due to the horizontal direction of motion, the joint contributions on the longitude (ϕ) motion have the largest amounts. As expected, the contributions of elbow flexion δ are negligible and the longitude motion of hand path geometry is dominated by the shoulder azimuth β. For the arm posture selection, the humeral rotation γ regulates the roll motion ψ. In order to observe the effects of elbow constraint, the same subject's non–constraint TH motion data is implemented in (18) and the joint DOF contributions are computed as shown in Figure 6(d–f). By comparing the Figure 6(b and e), we can find that the elbow DOF contributions on the hand path formulation are compensated by the humeral rotation γ. This can be intuitively interpreted that the CNS governs the joint motions along the determined hand path to reduce the required kinetic energy of the limbs. For the non–constraint condition, forearm motion (i.e. elbow motion) is actively involved due to its lower cost than the whole arm motion (i.e. shoulder involved motion) in terms of kinetic energy. As the elbow kinematics is locked in place, relatively large contribution of γ is incorporated due to different arm link moment of inertia with respect to the axis of rotation. Note that the required rotational energy will be reduced if the axis of rotation is aligned with the upper arm link's longitudinal axis (i.e. axis of γ rotation). Therefore, the humeral rotation γ is significantly involved both in the hand path geometry formulation and the arm posture selection.

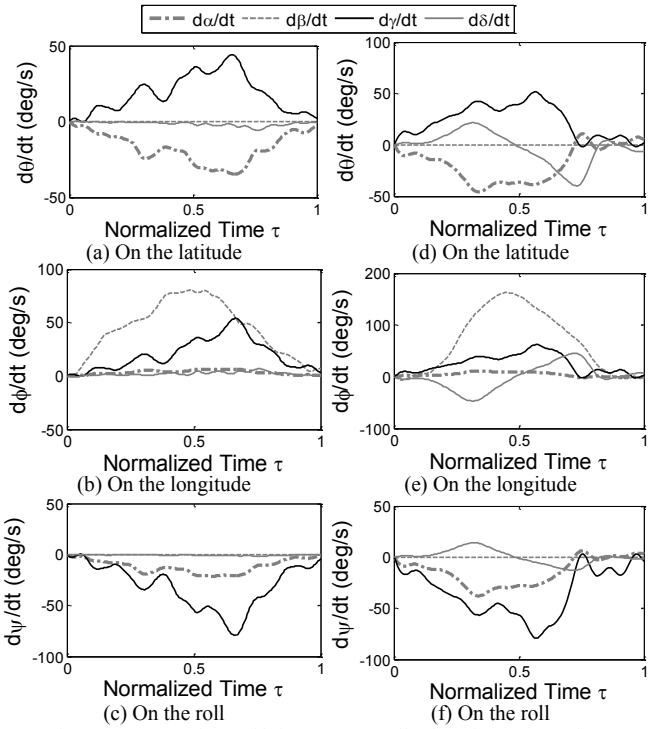

Figure 6. Comparison of joint DOF contributions in a TH motion: (a-c) show the constraint case while (d-f) present the non–constraint case

IV. Conclusion

From the presented experimental observations, we conclude that the point–to–point reaching with an elbow joint constraint can be approximated as the shortest path (i.e. Euclidean geodesic) between two positions on the constraint workspace. According to a quantitative analysis, the deviation between the experimental hand path and the geodesic curve was within 5% in terms of arc length. The speed profile of the hand motion roughly follows a smooth bell–shape which can be represented by the minimum jerk model output. With regard to the arm postural configuration, we found that the humeral rotation γ is actively involved in the reaching task with an elbow restrained arm. We believe that this phenomenon emerges to minimize the kinetic energy of the limbs. Extensive investigations on postural configurations under constrained joint conditions will be carried out in our future research.

References

[1] N. A. Bernstein, *The Co-ordination and Regaulation of Movements*. Oxford: Pergamon Press, 1967.

[2] M. D. K. Breteler and R. G. J. Meulenbroek, "Modeling 3D Object Manipulation: Synchronous Single-Axis Joint Rotations?," *Experimental Brain Research,* vol. 168, pp. 395-409, 2006.

[3] V. B. Brooks, *The Neural Basis of Motor Control*. New York: Oxford University Press, 1986.

[4] P. Morasso, "Spatial Control of Arm Movements," *Experimental Brain Research,* vol. 42, pp. 223-227, 1981.

[5] T. Flash and N. Hogan, "The Coordination of Arm Movements: An Experimentally Confirmed Mathematical Model," *The Journal of Neuroscience,* vol. 5, pp. 1688-1703, 1985.

[6] A. Biess, *et al.*, "A Computational Model for Redundant Human Three-Dimensional Pointing Movements: Integration of Independent Spatial and Temporal Motor Plans Simplifies Movement Dynamics," *The Journal of Neuroscience,* vol. 27, pp. 13045-13064, 2007.

[7] D. Sha, *et al.*, "Minimum Jerk Reaching Movements of Human Arm with Mechanical Constraints at Endpoint," *International Journal of Computers, Systems, and Signals,* vol. 7, pp. 41-50, 2006.

[8] D. G. Liebermann, *et al.*, "Planning Maximally Smooth Hand Movements Constrained to Nonplanar Workspace," *Journal of Motor Behavior,* vol. 40, pp. 516-531, 2008.

[9] X. Wang, "Three-Dimensional Kinematic Analysis of Influence of Hand Orientation and Joint Limits on the Control of Arm Postures and Movements," *Biological Cybernetics,* vol. 80, pp. 449-463, 1999.

[10] J. E. Richardson and T. Flash, "Comparing Smooth Arm Movements with the Two-Thirds Power Law and the Related Segemented-Control Hypothesis," *The Journal of Neuroscience,* vol. 22, pp. 8201-8211, 2002.